

Submitted as an **Original Article** to *Journal of Polymer Science Part A: Polymer Chemistry*

SP-PLP-EPR Investigations into the Termination Kinetics of *n*-Butyl Acrylate Macromonomers

Johannes Barth,¹ Michael Buback,¹ Christopher Barner-Kowollik,² Thomas Junkers,³
Gregory T. Russell^{4,*}

¹ Institute for Physical Chemistry, University of Göttingen, Tammannstr. 6, D-37077
Göttingen, Germany

² Preparative Macromolecular Chemistry, Institut für Technische Chemie und
Polymerchemie, Karlsruhe Institute of Technology, Engesserstr. 18, D-76128 Karlsruhe,
Germany

³ Polymer Reaction Design Group, Institute for Materials Research, Universiteit Hasselt,
Agoralaan, B-3590 Diepenbeek, Belgium

⁴ Department of Chemistry, University of Canterbury, Private Bag 4800, Christchurch, New
Zealand

* Corresponding author: E-mail: greg.russell@canterbury.ac.nz; Fax: +64 3 3642110

Keywords: ESR/EPR; kinetics (polym.); macromonomers (acrylate); mid-chain radicals; radical polymerization; termination

Abstract

The termination of model mid-chain radicals (MCRs), which mimic radicals that occur in acrylate polymerization over a broad range of reaction conditions, has been studied by single-pulse pulsed-laser polymerization (SP PLP) in conjunction with electron paramagnetic resonance (EPR) spectroscopy. The model radicals were generated by initiator-fragment addition to acrylic macromonomers that were preformed prior to the kinetic experiments, thus enabling separation of termination from the propagation reaction, for these model radicals propagate sparingly, if at all, on the timescale of SP-PLP experiments. Termination rate coefficients of the MCRs were determined in the temperature range 0–60 °C in acetonitrile and butyl propionate solution as well as in bulk macromonomer over 0–100 °C. Termination rate coefficients slightly below those of the corresponding secondary radicals were deduced, demonstrating the relatively high termination activity of this species, even when undergoing

MCR-MCR termination. For chain length 10, a reduction by a factor of 6 is observed. Unusually high activation energies were found for the termination rate coefficient in these systems, with 35 kJ mol^{-1} being determined for bulk macromonomer.

Introduction

Nowadays it is undisputed that reaction steps associated with mid-chain radicals (MCRs) play an important role in both conventional and reversible-deactivation ('controlled/living') radical polymerization (RP) of acrylates.¹ Indeed, any work on acrylate RP that did not consider the role of MCRs would not be taken seriously. And yet, remarkably, it was only just over a decade ago that the occurrence of MCRs in RP of acrylates was first proven definitively: Ahmad et al. used ^{13}C NMR to show the existence of branch points in poly(*n*-butyl acrylate),² and then a year later Chiefari et al. showed that high-temperature acrylate RP produces macromonomers in high yield.³ These works may be taken as proof, explicit and implicit, respectively, of the occurrence of chain transfer to polymer in these systems.

Progress since this breakthrough has been swift, with longstanding conundrums being cleared up. For example, the strongly non-classical variation of rate of polymerization with monomer concentration, c_M , that is observed in acrylates is now known to be a consequence of MCR formation followed by slow propagation⁴ – in effect there is increasing self-retardation as c_M becomes smaller. Similarly explained is the apparent variation of propagation rate coefficient, k_p , with pulsing frequency in pulsed-laser polymerization (PLP) experiments.⁵

These manifestations of MCR formation naturally elicit curiosity about how MCRs behave. Specifically, what reactions do they undergo and what values are taken by the rate coefficients for these reactions? Such information is essential for modeling the all-important quantities of rate of polymerization, molar mass distribution and branching level. It is now well accepted that MCRs may potentially undergo all of termination, β -scission, addition – to monomer, to RAFT agent in RAFT polymerizations, and so on – and even halide transfer, e.g. in ATRP systems.¹ However, while it is relatively easy to write down all these reactions, it has proven elusive to measure many of the associated rate coefficients. In the absence of such information, modeling becomes guesswork.

Especially for termination there is this vexing situation of rate coefficients being difficult to measure. It is easy to explain why: the simultaneous presence of secondary propagating

(chain-end) radicals (SPRs) means that there are three different termination processes occurring at once, namely homo-termination of SPRs, rate coefficient $k_t(\text{SPR},\text{SPR})$, homo-termination of MCRs, $k_t(\text{MCR},\text{MCR})$, and cross-termination between the two types of species, $k_t(\text{SPR},\text{MCR})$. Originally it was hoped that the so-called SP-PLP-EPR technique, which couples single-pulse (SP) PLP experiments with EPR spectroscopy,^{6,7} might solve this problem, not just because it is the most powerful technique for studying termination kinetics,⁸ but also by virtue of its ability to resolve the SPR and MCR populations and separately monitor their evolution with time.⁹ However this hope proved to be in vain, because it was found that the dominant impact of SPR-MCR cross-termination renders MCR-MCR termination difficult to assess.¹⁰ A similar problem arises with the β -scission (i.e., fragmentation) of MCRs, for which the significant contribution of MCR propagation prevents access to the much lower β -scission rate from SP-PLP-EPR data. Nevertheless, acrylate MCR fragmentation rates and activation energies, derived via other means, have been reported.¹

In view of this situation, it appeals to circumvent these difficulties by finding a model system for study of MCR termination kinetics in which interference by SPRs and by propagation does not occur. Such a system should be afforded by addition of primary radical fragments, denoted Init^{A} and Init^{B} , from photoinitiator decomposition, to acrylate-type macromonomers (MM): as is shown in Scheme 1, this generates tertiary radical species that are similar to the MCRs occurring during acrylate RP. The model MCRs, $\text{Init}^{\text{A}}\text{-MM}\cdot$ and $\text{Init}^{\text{B}}\text{-MM}\cdot$ (see Scheme 1) should be able to cross-propagate in the presence of an acrylate,¹¹ just as conventional MCRs add to monomer in acrylate homopolymerizations. However, on account of the large steric hindrance it is not expected that these model MCRs can add to MM on the timescale of an SP-PLP experiment. This has been confirmed by SEC and by mass-spectrometric analysis of an MM reaction mixture before and after treatment with a thermal initiator up to complete decomposition: no observable increase in polymer size occurs.¹²

Such an observation is consistent with the measured k_p for the so-called methyl acrylate¹³ and butyl acrylate¹⁴ dimers, which are about a factor of 1 000 lower than k_p for the corresponding acrylates. Specifically, for the BA dimer the average time that is required for a propagation step to take place is roughly 1 s at 20 °C (under the conditions of the present macromonomer experiment in 10% solution assuming an average molecular weight of 2 000 g mol⁻¹). Thus, on the timescale of the experiments outlined herein, a little propagation would occur with the dimer. However, the BA dimer value may be considered as an upper bound for present purposes, as reduced propagation rates must be expected when increasing the size of the

macromonomer to chain length 3 or above. So no significant propagation is expected in our experiments. Incidentally, the fact that steric hindrance is responsible for reduced propagation rate coefficients certainly engenders an expectation of reduced termination rate coefficients for macromonomers on account of the same cause.

As it so happens, acrylate macromonomers are readily obtainable as a result of recent intensive study,^{15,16} indeed Barner-Kowollik and Junkers prepared a library of such species.¹⁷ Accordingly, in this work samples of *n*-butyl acrylate (BA) MM will be examined via SP-PLP-EPR.⁶ As just explained, the resulting radicals should be models for acrylate MCRs formed by backbiting (i.e., intramolecular chain transfer to polymer), and they should not readily propagate. Thus, to a good approximation, the decay in radical concentration, c_R , that is consequent upon a laser pulse should be given by

$$\frac{dc_R}{dt} = -2k_t(c_R)^2 \quad (1)$$

where the k_t is for a termination process that mimics MCR homo-termination. For this reason the k_t obtained from such SP-PLP-EPR experiments should be representative of $k_t(\text{MCR}, \text{MCR})$ values in acrylate RP. This, then, is what will be done in the present work.

Experimental Section

BA macromonomer (MM) was synthesized as described elsewhere.¹⁷ The solvents acetonitrile (AN; Sigma-Aldrich, 99.8%) and butyl propionate (BP; Aldrich, 99%) were used as received. Solutions of macromonomer and solvent were degassed by several freeze-pump-thaw cycles. The photoinitiator α -methyl-4(methylmercapto)- α -morpholinopropiophenone (MMMP; Aldrich, 98%) was used as received. It was added to solution in a glove box under an argon atmosphere to yield MMMP concentrations of $1.5 \times 10^{-2} \text{ mol L}^{-1}$. Sample volumes of 0.05 mL were filled into quartz tubes of 3 mm outer and 2 mm inner diameter.

The tubes were fitted into the EPR resonator cavity of a Bruker Elexsys E 500 series cw-EPR spectrometer. The samples were irradiated through a grid by a COMPex 102 excimer laser (Lambda Physik) operated on the XeF line (351 nm). The laser energy per pulse was around 80 mJ. The EPR spectrometer and the laser source were synchronized by a pulse generator (Scientific Instruments 9314). Temperature control was achieved via an ER 4131VT unit (Bruker) by purging the sample cavity with nitrogen. The decay in radical concentration after

applying a single (laser) pulse at $t = 0$ was monitored via the EPR intensity at fixed magnetic field. To improve signal-to-noise quality, up to 10 individual $c_R(t)$ traces were co-added. EPR intensity was calibrated for absolute radical concentration via the procedure described elsewhere^{6,18} that involves the stable radical compound 2,2,6,6-tetramethyl-1-piperidinyloxy (TEMPO; Aldrich, 99%), which was used without further purification. The entire experimental procedure has been described in greater detail in previous work on SP-PLP-EPR.⁶

The SP-PLP-EPR experiments were carried out at temperatures between 0 and 100 °C for bulk macromonomer and for MM dissolved in both BP and AN at MM weight fractions of between 10 and 85 percent.

Results and Discussion

Demonstration of concept. The EPR spectrum observed during continuous irradiation of a reaction mixture consisting of MM and MMMP is shown in Figure 1. As illustrated, the EPR signal for the model MCRs is found to be more or less identical to the spectrum recorded during an acrylate polymerization at 70 °C, where the fraction of MCRs is close to 90 %.⁹ This may be taken as proof of the idea behind this work, i.e., that SP-PLP experiments involving MM as monomer will give information about MCR termination.

Having said that, there are some minor differences in the splitting patterns of the EPR spectra shown in Figure 1, i.e., those from this work and from BA MCRs in the earlier work.⁹ These arise from: (1) Restricted rotation around the carbon bond next to the radical functionality, which is more pronounced in the more viscous macromonomer system;⁹ and (2) Small variation in coupling constants due to the difference between the initiator fragments and an acrylate monomer unit.

Data analysis. For SP-PLP-EPR measurement on the MM/MMMP system, the intensity of the large, central EPR line of the MM signal – see the left-hand side of Figure 1 – was monitored after applying an intense laser pulse. From this intensity, the radical concentration, c_R , was obtained as a function of time, t . These traces were fitted to Equation (2), which follows from integration of the termination rate law, Equation (1):^{8,19}

$$\frac{c_R(t)}{c_R(0)} = (2k_t t c_R(0) + 1)^{-1} \quad (2)$$

In this equation, $c_R(0)$ denotes the MCR concentration produced by addition of initiator fragments to MM directly after applying a laser SP at $t = 0$. This quantity is yielded by the EPR procedure. So the only variable in the fitting is k_t , the value of which is thus delivered by this procedure. Equation (2) assumes there is no change of k_t with time. If there is, then the fitting of Equation (2) yields a time-averaged termination rate coefficient, $\langle k_t \rangle$. The fitting procedure is illustrated in Figure 2 for radical traces obtained with bulk MM at 0 and 80 °C.

It should be no surprise from the above that the major source of experimental uncertainty in k_t is error in $c_R(0)$.⁶ As detailed elsewhere,^{6,18} this has a number of causes, including: concentration and filling level of TEMPO (used for calibration) and MM solutions; and mathematical processing of the experimental EPR spectra, viz. baseline adjustment and integration steps. The resulting error in k_t is conservatively estimated to be 30%.^{6,18,20} Note that there is also variation in $c_R(0)$ from experiment to experiment, even under ostensibly identical conditions.⁶ This variation is typically 30–50%, and is a consequence of differences in laser light intensity and, at low temperatures, of condensation of water on the sample-tube surface. On top of this there is variation of $c_R(0)$ due to solvent amount. In our experiments we at all times obtained physically realistic values of $c_R(0)$, and we found no correlation between scatter in k_t values and variation of $c_R(0)$ values. This gives confidence that the error in our k_t is random rather than systematic.

Non-ideality of fits. The fits by Equation (2), which are represented by the gray lines in Figure 2, deviate from the experimental $c_R(t)$ data in a systematic manner. Termination of model MCRs proceeds with higher rate coefficient at short times after applying the laser SP and with lower rate coefficient at longer t . This can be deduced from the fact that the best fits lie above the data at early times (i.e., the best-fit k_t is too small) and below the data at late times. This is shown formally in Figure 3, which presents fits of Equation (2) over discrete time intervals. Specifically, Equation (2) is fitted where $c_R(t) > 0.35 \times c_R(0)$ and then separately for $c_R(t) < 0.35 \times c_R(0)$ (long times). It is found that k_t from the early-time fitting is higher by a factor of 5 than k_t from the long-time fitting, i.e., there is a clear decrease of k_t during the course of an SP-PLP. A number of suggestions occur for explaining this situation; four of these – by no means an exhaustive list – will now be discussed in turn.

1. Chain-length-dependent termination due to radical growth. The termination rate coefficient of the model MCRs appears to decrease with time after pulsing. Such a decrease in k_t has been observed in all SP-PLP-EPR results to date,^{6,20,21} and has been uncontroversially assigned to chain-length-dependent termination (CLDT).^{6,22} as the radicals grow during the time period of

the experiment, k_t declines. However, this explanation is highly unlikely to be applicable for macromonomers, which are expected to propagate too slowly^{13,14} on the timescale of SP-PLP-EPR measurements for any significant growth in chain length to occur.¹² That said, the door should not be fully closed on this suggestion until it has been specifically investigated.

2. *Temperature.* Inspection of the $c_R(t)$ traces in Figure 2 seems to indicate that increasing temperature allows for better fitting with Equation (2), i.e., a single k_t value becomes more appropriate as temperature is raised, and thus one should search for an explanation for non-ideality that is related to temperature. However Figure 4 exposes such thinking as spurious: it is shown that when the data of Figure 2 are re-plotted so that the timescales are kinetically equivalent, the deviations from ideality are more-or-less the same. In other words, the impression from Figure 2 that the 80 °C is better described by Equation (2) is an optical illusion created by the much lower relative radical concentration that is reached, due to the higher k_t , on the timescale of the experiment. In view of this it may be said that results are non-ideal at all temperatures, and that deviations from ideality are not due to a side-reaction that becomes less influential at higher temperature.

3. *Chain-length-dependent termination due to macromonomer polydispersity.* As shown in Figure 5, the utilized macromonomer sample is polydisperse: it is known^{15,17} that BA macromonomers with degree of polymerization between 3 and about 50 are contained in the initial MM sample of average chain length about 10. Kinetic simulations have shown that such polydispersity is an unavoidable consequence of the formation chemistry.²³ Making the reasonable assumption that macromonomers of all sizes react with the MMMP fragments Init^A and Init^B (see Scheme 1) at a rate that is fast on the timescale of termination, our SP-PLP-EPR experiments therefore must have had a chain-length distribution of radicals at $t = 0$ that mirrors the size distribution of the initial MM mixture, as shown in Figure 5. Given that this distribution is polydisperse and that there is no obvious reason why macromonomer radicals should not display chain-length-dependent termination, one therefore must expect that our macromonomer sample was characterized by a spectrum of termination rate coefficients, which is contrary to what Equation (2) assumes. Note that this situation may sound similar to that of standard monomers with SP-PLP-EPR, but in fact it is different: in the usual situation there is decrease of k_t with t as the (relatively) monodisperse radical population propagates to become longer in size, whereas in the present case there are different but fixed radical sizes present at all times. Thus the equations used to account for CLDT in SP-PLP-EPR experiments²⁴ are not applicable.

Given this, we conducted simulations with the PREDICI[®] software package²⁵ to investigate the effect of radical polydispersity on SP-PLP-EPR kinetics. The input distribution of radical sizes was the measured one of Figure 5. The total initial MCR concentration was set to $c_R(0) = 1 \times 10^{-5} \text{ mol L}^{-1}$, a typical order of magnitude for this quantity. The so-called composite model for termination²⁶ was employed:

$$k_t^{i,i} = k_t^{1,1} i^{-\alpha_s}, \quad i \leq i_c$$

$$k_t^{i,i} = k_t^{1,1} (i_c)^{-\alpha_s + \alpha_1} i^{-\alpha_1} \equiv k_t^0 i^{-\alpha_1}, \quad i > i_c \quad (3)$$

Equation (3) has been found to describe CLDT in essentially all systems investigated to date.^{6,22} BA literature values^{10,20} of the long-chain exponent, α_1 , and the crossover chain length, i_c , were adopted here. Note that these values are of very low importance, as the average degree of polymerization of the MM sample under investigation is about 10 (see Figure 5), which is well below the average acrylate value for i_c of 30.²⁰ This means that the vast majority of termination events involve ‘small’ radicals, and so the parameters α_s , the so-called small-chain exponent, and $k_t^{1,1}$, the rate coefficient for termination between two species with $i = 1$, are crucial. For chain-end radicals in acrylate polymerization, an average value of $\alpha_s = 0.79$ has been found.²⁰ For acrylate MCRs this value may be different; on the basis of long-chain studies one might expect it to be slightly higher for radical functionality a little removed from the chain end.²⁷ However the value should not exceed unity.²¹ Therefore we decided to use $\alpha_s = 1$, as this should give maximum possible effect for the idea under consideration, and hence indicate whether it is at all a possible explanation for the non-ideality of our $c_R(t)$ traces. (Note that by now CLDT is considered to be normal;^{6,22} the term ‘non-ideal’ should be interpreted to mean ‘not fitted by Equation (2)’, rather than that there is anything unusual about CLDT.)

Simulation results are presented in Figure 6. The geometric-mean model was employed for cross-termination:

$$k_t^{i,j} = (k_t^{i,i} k_t^{j,j})^{0.5} \quad (4)$$

The value $k_t^{1,1} = 1 \times 10^6 \text{ L mol}^{-1} \text{ s}^{-1}$ was chosen as it was found to give a good match between simulation output and measured signal trace for bulk MM at 40 °C, as is evident from Figure 6. This figure shows that while the best fit of the data to Eq. (2) (dashed line) has the above described deviation from ideality, an improved match is obtained with the simulation data

(full line), in fact radical concentrations at longer delay times are very well reproduced. At short times after the laser pulse a somewhat faster decay in radical concentration is still observed in the experiment compared with the simulation. Despite the fact that a slightly higher starting radical concentration was assumed for simulation compared with the experimental trace, the simulation gives a good qualitative indication that chain-length dependence contributes to the identified non-idealities.

In physical terms, what is happening here? Because of the faster termination of small radicals, the chain-length distribution of the model MCRs varies with time after applying the laser pulse at $t = 0$. Specifically, there is a gradual shift in MM size distribution towards longer chain lengths, as the smaller radicals preferentially terminate, and this shift causes $\langle k_t \rangle$, the average over all chain lengths, to decrease as time proceeds.

Incidentally, note that the best-fit k_t for the simulation results is extremely close in value to $k_t^{1,1} \times DP_n^{-\alpha_s}$ (cf. Equation (3)), where $DP_n \approx 10$ is the number-average degree of polymerization of the MM sample (see above). Such an outcome should not come as a surprise to those familiar with the theory of CLDT,²² and is a useful result that will shortly be exploited.

4. Kinetically distinct macroradicals from photoinitiation. The photoinitiator MMMP dissociates into two structurally different fragments, hence in principle two chemically distinct species are available for termination in this work, viz. $\text{Init}^{\text{A}}\text{-MM}\cdot$ and $\text{Init}^{\text{B}}\text{-MM}\cdot$ (see Scheme 1). It is conceivable that these two species could have quite different termination reactivity, because the pendant group can markedly influence k_t via steric effects.^{6,22} For example, highly hindered monomers such as butyl acrylate dimer,¹⁴ di-*n*-butyl itaconate²⁸ and dimethyl itaconate²⁹ have been found to have k_t about 1–2 orders of magnitude lower than equivalent monomers without such steric hindrance.¹⁴ If such an effect is occurring with $\text{Init}^{\text{A}}\text{-MM}\cdot$ and $\text{Init}^{\text{B}}\text{-MM}\cdot$, then it may give rise to non-ideality in $c_{\text{R}}(t)$ traces.

To investigate this idea, further simulations with PREDICI[®] were carried out. Figure 7 presents results from using $k_t(\text{A,A}) = 1 \times 10^5 \text{ L mol}^{-1} \text{ s}^{-1}$, $k_t(\text{A,B}) = 1 \times 10^4 \text{ L mol}^{-1} \text{ s}^{-1}$, and $k_t(\text{B,B}) = 5 \times 10^3 \text{ L mol}^{-1} \text{ s}^{-1}$, where A and B denote $\text{Init}^{\text{A}}\text{-MM}\cdot$ and $\text{Init}^{\text{B}}\text{-MM}\cdot$ respectively. As earlier with $k_t(\text{SPR,SPR})$, etc., a different notation to k_t^{ij} is used so as to convey that the variation here in individual k_t is not due to chain length. In effect this model is just a simplified version of CLDT, where now there are only two states ('A' and 'B') rather than all possible chain lengths, and both states start off with equal population, as opposed to the

complicated starting distribution of Figure 5. Having initially equal concentrations of A and B species assumes that both photoinitiator fragments add equally well to the MM and that no persistent (initiator-derived) radical is present.

Of course the given values of $k_t(A,A)$, $k_t(A,B)$ and $k_t(B,B)$, while plausible, are nevertheless somewhat arbitrary, as they must be in the absence of hard-and-fast data. With different values for these parameters one can obtain varying degrees of non-ideality in $c_R(t)$ traces. The results of Figure 7 are simply those from a set of not unreasonable k_t values that yield $c_R(t)$ qualitatively similar to our experimental data. That the latter is the case can be seen by comparing Figure 7 with earlier figures in which fits of Equation (2) to experimental data are presented: the deviations are of the same magnitude and nature. This shows that the present model is capable of explaining the experimental data. This would be even more so the case were further chemical subtleties to be incorporated into modeling, for example that $\text{Init}^A\text{-MM}\cdot$ and $\text{Init}^B\text{-MM}\cdot$ may form on different timescales as a result of the photoinitiator fragments Init^A and Init^B adding to MM at significantly different rates, or that Init^A and Init^B may have different rates of self-termination, which also will give rise to disparate concentrations of $\text{Init}^A\text{-MM}\cdot$ and $\text{Init}^B\text{-MM}\cdot$ – clearly there are many possibilities for further investigation if desired.

It is also important to note about the simulation results of Figure 7 that when fitted by Equation (2), they yield an overall k_t that is representative of the input termination rate coefficients.

Summation. Two plausible models have been found for qualitatively explaining the non-ideality in our $c_R(t)$ traces, indeed it is quite possible that both effects may play a role in reality. Certainly the CLDT explanation should be operative, because it is based on well-established facts, namely that the starting MM distribution is polydisperse and that termination is chain-length dependent. However the investigative simulation of this work adopted what is considered to be the strongest possible extent of CDLT (viz. $\alpha_s = 1$), and yet the resulting deviation from ideality may not be as strong as that observed in experiments (see Figure 6). Hence it may be that markedly different termination rate coefficients for $\text{Init}^A\text{-MM}\cdot$ and $\text{Init}^B\text{-MM}\cdot$ – most likely as a result of steric effects – are an extra cause of non-ideality in $c_R(t)$ to a significant extent. There is much scope, through altered parameter values and extra mechanistic subtleties (some of which have been mentioned), for obtaining better quantitative agreement with the data. Our main intention here has just been to show qualitatively that this is possible, which we believe we have done.

Be all this as it may, the most important point here is that even though Equation (2) does not perfectly fit our experimental $c_R(t)$ traces, it has been established that these non-idealities may be explained within a conventional termination framework, and that the k_t values obtained from fitting Equation (2) are still representative of the termination processes occurring. Thus one may be confident that the MM system under investigation is well suited for studying MCR kinetics via SP-PLP-EPR.

Results. Arrhenius plots of k_t values of this work – as procured from best-fitting of Equation (2) to SP-PLP-EPR data – are presented in Figure 8. Values of Arrhenius parameters are listed in Table 1, as obtained from (straight-line) Arrhenius fits. For bulk MM and for the most dilute MM solution (10 wt.% in butyl propionate, BP), temperature was varied between 0 and 100 °C. No Arrhenius fit is given for 10 wt.% MM in BP, as the scatter in the measured data, in particular at higher temperature, is significant. For the two intermediate dilutions of MM, the temperature range was 0 to 60 °C, and so fewer data points were obtained; further, in the case of the MM mixture containing 15 wt.% acetonitrile (AN), an outlier point was omitted from Arrhenius fitting (see Table 1 footnotes for details). BP was used as a solvent because it is the saturated analogue of BA, the significance of which will shortly be seen; AN was employed because it is a common (co-)solvent in ATRP of acrylates, and so the resulting k_t values may be of interest for ATRP modeling.

Discussion of results. Firstly, there is no evident curvature in the Arrhenius plots of Figure 8. If a side reaction such as β -scission, which has a relatively high activation energy, were coming into play at higher temperature, then the resulting SPRs would be expected to terminate more quickly than MCRs, thereby giving rise to a higher system k_t , and thus to non-Arrhenius behavior in $\log k_t$ vs. T^{-1} . That this is not observed gives confidence that the measured decay of c_R with t is entirely (or at least largely) due to MCR termination under all conditions.

Next we consider the activation energies of Table 1. These E_a values are unusually high. In previous SP-PLP-EPR work, it has consistently been found that the measured $E_a(k_t^{1,1})$ is equal, within experimental error, to the measured $E_a(\eta^{-1})$, where η denotes the viscosity of the monomer-solvent system.^{6,20,21} This is as expected for a diffusion-controlled reaction between small molecules. Unfortunately, η as a function of temperature, and hence $E_a(\eta^{-1})$, are not available for the bulk MM and MM/solvent systems of this work. However what may be said is that the MM samples used in this work are highly viscous by small-molecule norms, exactly as one would expect of MM (which, after all, is small polymer). Thus it cannot be

excluded that $E_a(\eta^{-1})$ may approach values as high as the $E_a(k_t)$ measured here for bulk MM. Furthermore, one notes that our $E_a(k_t)$ seem to decline towards more normal small-molecule values of $E_a(\eta^{-1})$ as solvent is added, which is as one would expect for diffusion control, although one cannot be sure that this trend is really present in the data, because the variation of E_a is within the limits of experimental uncertainty (see Table 1). In fact the closeness of the $E_a(k_t)$ for bulk MM and for 20 wt.% MM in butyl propionate suggests that reduced segmental mobility due to steric hindrance is the more likely explanation for the $E_a(k_t)$ being as high as they are. Large activation energies, e.g., of about $E_a(k_t^{1,1}) = 28 \text{ kJ mol}^{-1}$, have already been measured for di-*n*-butyl itaconate and assigned to the impact of steric shielding^{14,28} (although admittedly this was also in the absence of any information on solvent viscosity).

Considering now the values of k_t , we first of all note that the relative ordering is as one would expect on the basis of diffusion control: as η decreases in changing from 100% (bulk) MM to 85% MM to 20% MM to 10% MM, k_t increases (see Figure 8). At 30 °C, for example, this increase in k_t amounts to more than 2 orders of magnitude.

In terms of absolute values, there are two comparisons we may make, both relating to our system of 10 wt.% MM in butyl propionate. This solvent was chosen because, as already mentioned, it is the saturated analogue of *n*-butyl acrylate, and so in physical terms it should mimic MM being surrounded by the analogous monomer. Thus it is reasonable to compare this data set with values from bulk BA polymerization.

The first comparison is with bulk BA values of $k_t^{10,10}(\text{SPR,SPR})$ (i.e., homo-termination of SPR 10-mers) at low conversion, as obtained in previous SP-PLP-EPR studies.^{10,20} This is the top line in Figure 8. The reason for choosing chain length 10 is that, as mentioned earlier, our derived k_t probably correspond reasonably closely to $k_t^{10,10}(\text{MCR,MCR})$ values. At 30 °C, our $k_t(\text{MCR,MCR})$ value for 10 wt.% MM in BP is about a factor of 6 lower than $k_t^{10,10}(\text{SPR,SPR})$ for BA (see Figure 8). Some of this difference can be assigned to higher viscosity due to the 10 wt.% MM. However it is highly unlikely that η changes can nearly explain the full extent of the difference. Thus these results suggest more steric shielding and reduced segmental mobility of the model MCRs in comparison with SPRs. This should not come as a surprise, because it is commonly accepted that MCRs have significantly lower k_t than equivalent SPRs,⁴ indeed if anything the surprise might be that the effect only seems to amount to about a factor of 5.

The second comparison is with chain-length averaged $k_t(\text{MCR},\text{MCR})$ from steady-state BA bulk polymerization. From carrying out detailed data analysis,³⁰ Nikitin and Hutchinson have estimated for this quantity:³¹

$$k_t(\text{MCR},\text{MCR}) = 1.8 \times 10^7 \text{ L mol}^{-1} \text{ s}^{-1} \exp[-5.6 \text{ kJ mol}^{-1} / (RT)] \quad (5)$$

Equation (5) gives $k_t = 2.0 \times 10^6 \text{ L mol}^{-1} \text{ s}^{-1}$ for 30 °C, as compared with $k_t = 1.4 \times 10^7 \text{ L mol}^{-1} \text{ s}^{-1}$ at 30 °C from using the Arrhenius parameters of Table 1 for 10 wt.% MM in BP. This is a difference of a factor of 7, which most logically is due to CLDT: MCR chain lengths are much larger in steady-state BA polymerization than in the present study (see Figure 5), resulting in lower k_t than found here.

Incidentally, the E_a of Equation (5) is noticeably lower than those of Table 1. In this context it is interesting that the most recent modeling study by Nikitin et al. recommends the quite different values of $A = 5.3 \times 10^9 \text{ L mol}^{-1} \text{ s}^{-1}$ and $E_a = 19.6 \text{ kJ mol}^{-1}$ for (chain-length averaged) $k_t(\text{MCR},\text{MCR})$ in steady-state BA solution polymerization.³² These values are more in line with those of the present work (see Table 1), but they still give essentially the same value as Equation (5) for 30 °C ($2.2 \times 10^6 \text{ L mol}^{-1} \text{ s}^{-1}$), meaning the argumentation above is unaffected.

From the two comparisons given here, it may be said that $k_t(\text{MCR},\text{MCR})$ from this work is perfectly consistent with values from similar but slightly different literature systems. This instills yet more confidence in the values from the present investigation.

Finally, we would like to stress that the Arrhenius fits of Figure 8 should not be used outside the temperature range of measurement; doing so may amongst other things lead to unjustified mechanistic conclusions.

Conclusion

Investigations into termination are rarely straightforward; invariably there are difficulties in explaining all aspects of the data.²² In this respect the present work is no exception, for example there has been the non-simple nature of $c_R(t)$ traces (in the sense that they are not adequately fit by Equation (2)) and the uncommonly high values of $E_a(k_t)$. Nevertheless, plausible explanations for these and all other features of our data have been found. What may not be noticed due to all this commotion is a simple but very important finding: how *normal*

are the k_t values we have found for our model chain-end MCR radicals. What we mean by this is how well they nestle in with literature values for BA systems and how comfortably they sit with current knowledge about termination. Certainly, acrylate-derived MCRs seem to have k_t values that are slightly lower than analogous SPRs, which is as one would expect. However, the values are not uncommonly lower, and our MCRs show a typical kind of termination kinetics²² without any anomalies.

In terms of future work, several doors have been opened. Most obviously, it would be useful to measure MM viscosities, to carry out SP-PLP-EPR experiments with monodisperse MM samples, and to use a photoinitiator that results in MCR species of essentially equal termination reactivity (as opposed to the speculation here that $\text{Init}^{\text{A}}\text{-MM}\cdot$ and $\text{Init}^{\text{B}}\text{-MM}\cdot$ have significantly different k_t). More adventurously, the present MM system might be used for estimates of MCR β -scission (i.e. fragmentation) rates at higher temperature. These experiments should preferably be carried out under conditions of low termination rate, i.e., in solution of a highly viscous compound such as naphthalin.

Acknowledgements: J. B. is grateful to the *Fonds der Chemischen Industrie* for a doctoral fellowship. G.T.R. thanks the University of Canterbury for provision of study leave, during which this project was carried out. C.B.-K. acknowledges continued support from the Karlsruhe Institute of Technology (KIT) in the context of the *Excellence Initiative* for leading German universities. T. J. is grateful for funding from the *Fonds Wetenschappelijk Onderzoek (FWO)* in the framework of the Odysseus scheme. The authors are grateful to Anna-Marie Zorn (KIT) for the provision of the macromonomer and to Joachim Morick (UoG) for support with some of the experiments.

Graphical Abstract

Model mid-chain acrylate radicals were generated by addition of primary initiating radicals to *n*-butyl acrylate macromonomer. The termination of these radicals was investigated via SP-PLP-EPR experiments, over the timescale of which the radicals do not propagate. Thus the measured k_t values should be indicative of those for actual acrylate mid-chain radicals, which are essentially impossible to isolate for kinetic study via conventional experiments. As shown, our MCRs were found to display typical termination behavior without any anomalies.

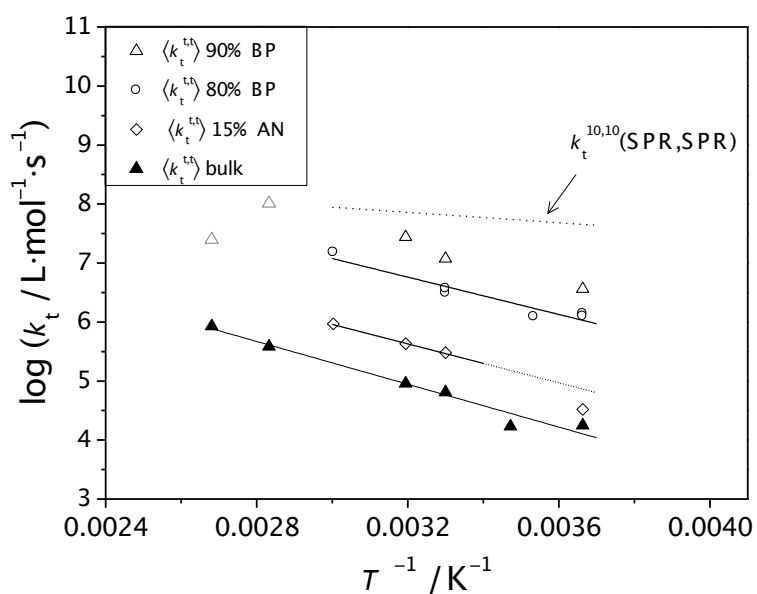
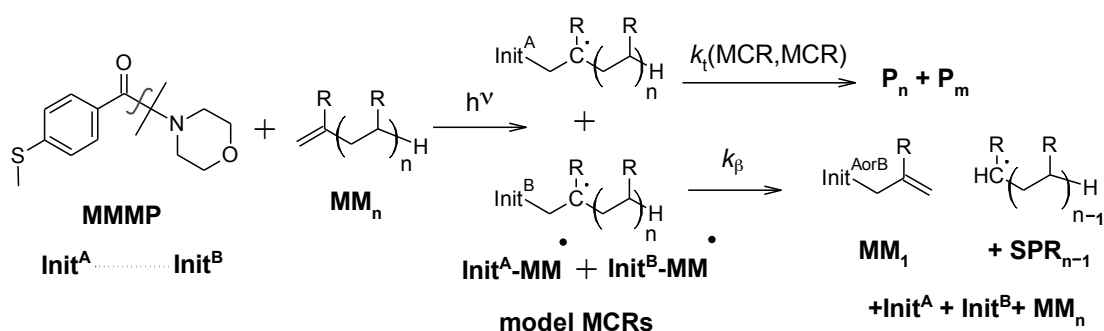


Table 1. Activation energy, E_a , and pre-exponential factor, A , for $k_t(\text{MCR}, \text{MCR})$ values of this work, as obtained from Arrhenius fits of Figure 8.

system ^{a)}	$E_a / \text{kJ mol}^{-1}$	$A / \text{L mol}^{-1} \text{s}^{-1}$	temperature range ^{b)}
bulk MM	35 ± 5	5.6×10^{10}	0 – 100 °C
85 wt.% MM in AN	32 ± 7	8.1×10^{10}	0 – 60 °C ^{c)}
20 wt.% MM in BP	30 ± 5	6.6×10^{11}	0 – 60 °C

^{a)} MM denotes BA macromonomer, AN acetonitrile and BP butyl propionate; ^{b)} Range of temperatures for which k_t was measured (see Figure 8), and therefore for which the given Arrhenius parameters hold; ^{c)} 0 °C point omitted from Arrhenius fit, as deemed an outlier (inspect Figure 8).



Scheme 1. Formation of model mid-chain radicals (MCRs) that can be used for studying MCR kinetics in the absence of secondary propagating radicals (SPRs). In this work the fragments Init^{A} and Init^{B} arise from UV-induced decomposition of the photoinitiator MMMP. These then add to the macromonomer (MM, where R is *n*-Bu-O-CO- in this work) to form model MCRs, which react either by termination (most likely via disproportionation) or, at temperatures well above 80 °C, by β -scission. The latter reaction is just the reverse of the addition reaction that forms the model MCRs in the first place.

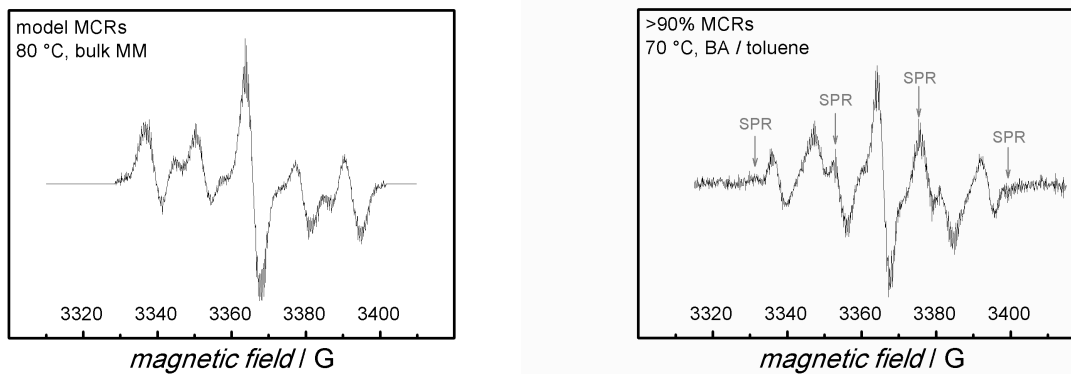


Figure 1. Spectra recorded during continuous photoinitiation of MMMP in bulk macromonomer (left-hand side; this work) and in BA solution (1.5 mol L⁻¹ in toluene; right-hand side⁹) at similar polymerization conditions and EPR settings. The low-intensity field positions associated with secondary propagating (chain-end) radicals (SPRs) are indicated on the right-hand spectrum, making clear that the signal is predominantly from mid-chain radicals (MCRs).⁹

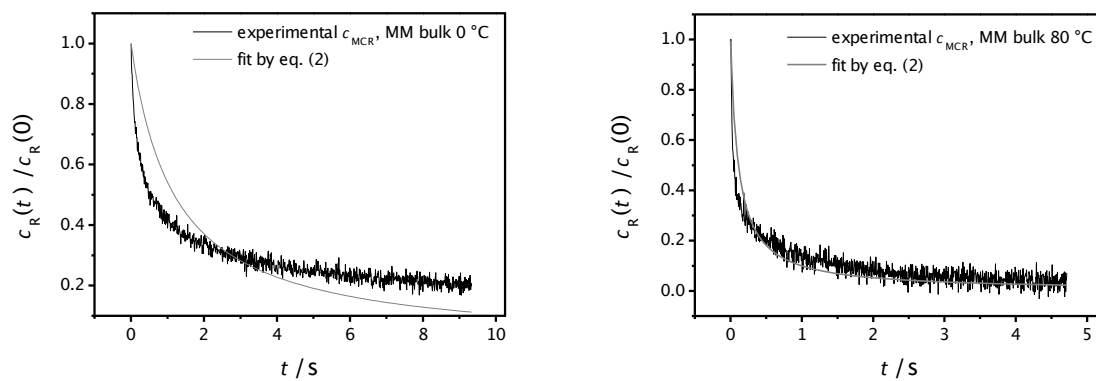


Figure 2. MCR concentration, c_R , versus time, t , at $0\text{ }^\circ\text{C}$ (left-hand side) and at $80\text{ }^\circ\text{C}$ (right-hand side) from SP-PLP-EPR experiments with BA macromonomer in bulk, where the initial MCR concentration, $c_R(0)$, has been determined by calibration. Traces: experimental data; curves: best-fits of Equation (2) to the data, yielding $k_t = 1.7 \times 10^4\text{ L mol}^{-1}\text{ s}^{-1}$ at $0\text{ }^\circ\text{C}$ and $8.5 \times 10^5\text{ L mol}^{-1}\text{ s}^{-1}$ at $80\text{ }^\circ\text{C}$.

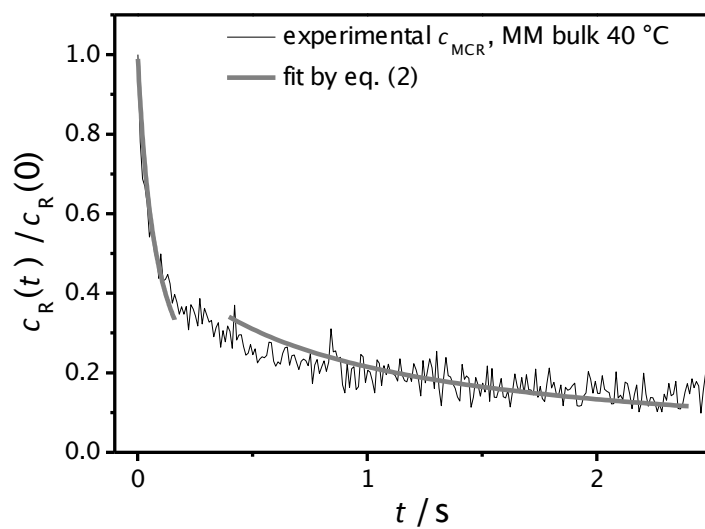


Figure 3. As for Figure 2, but with data from 40 °C, and carrying out separate fitting for shorter and for longer times (see text), where the division between the two regions has been (arbitrarily) set at 35% of the initial radical concentration. The early-time fit yields k_t that is half an order of magnitude larger than k_t from the late-time fit.

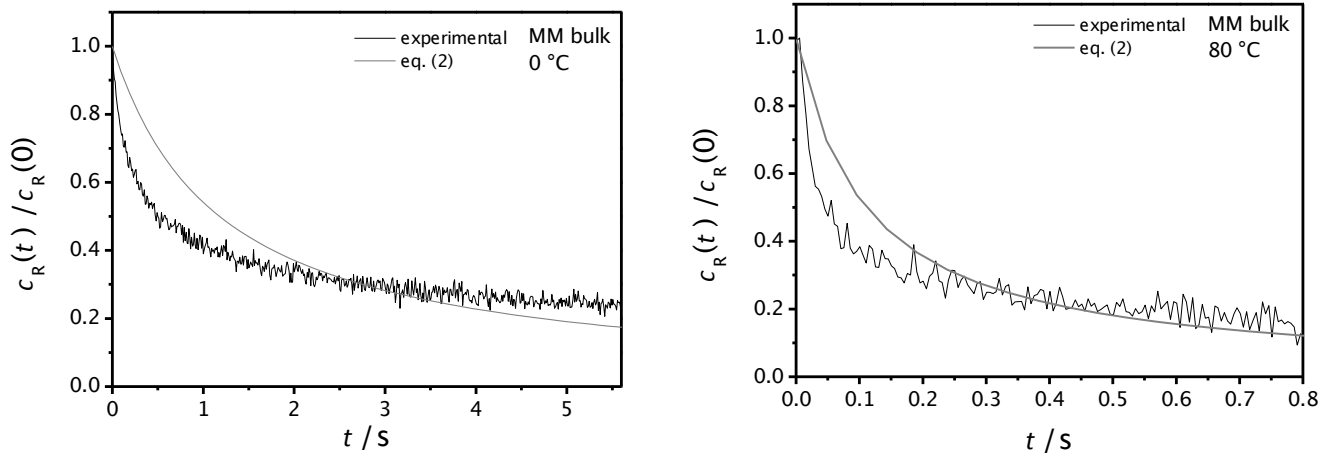


Figure 4. As for Figure 2, but presenting the data so that each intersection of the experimental data and the best fit of Equation (2) is located at the mid-point of the time axis.

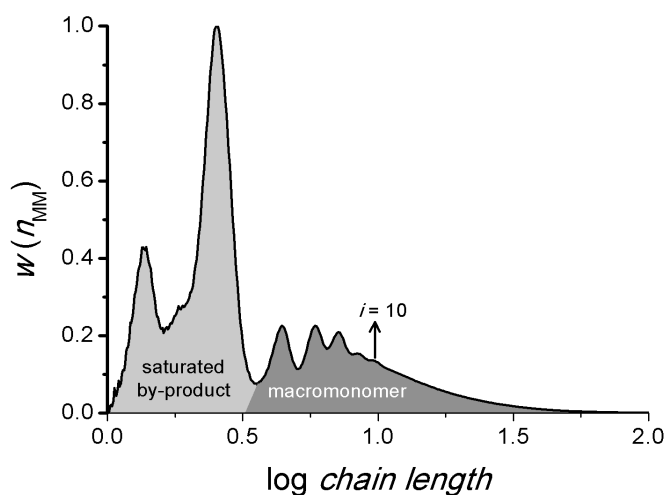


Figure 5. Number chain-length distribution of the butyl acrylate macromonomer sample^{15,17} used for the SP-PLP-EPR studies of this work. The chain-length distribution was obtained as part of the present work by size-exclusion chromatography with the calibration referring to poly(styrene) standards. The fraction of saturated by-product from macromonomer synthesis, shown as a light gray area, is that after reduction by distillation, done as part of the present work.

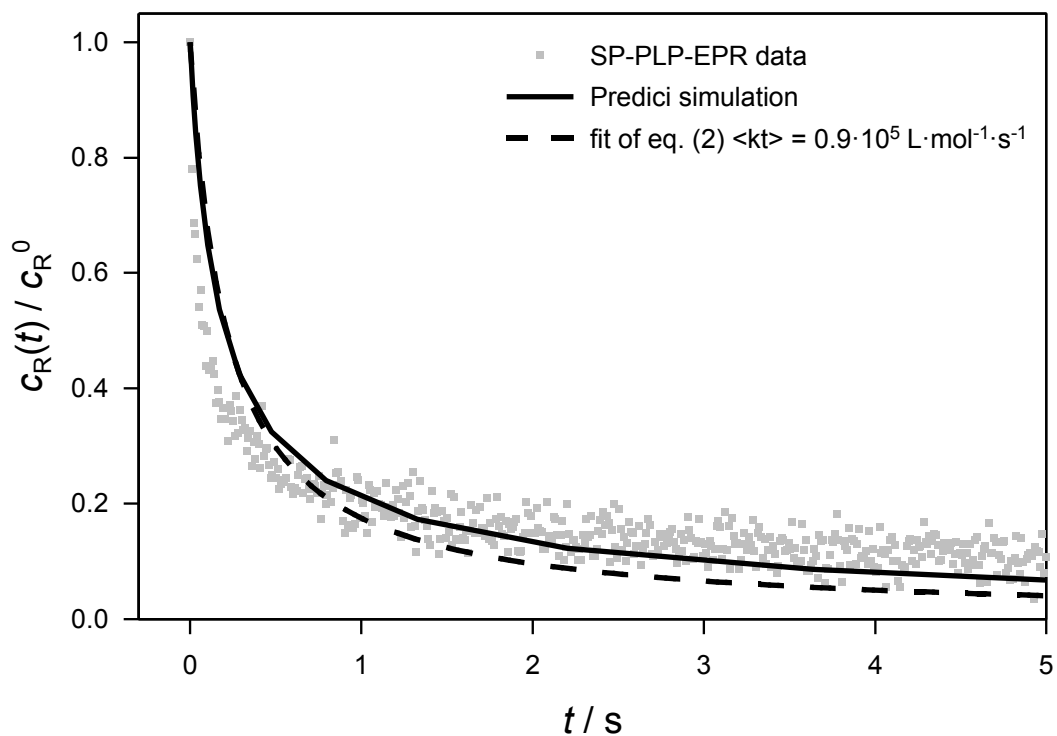


Figure 6. SP-PLP-EPR experimental results for bulk MM at 40 °C (points) (see Figure 2 for other temperatures but otherwise analogous conditions). The dashed line represents the best fit of the data to Eq. (2) while the full line is the improved match from a simulation taking chain-length-dependent termination into account with model and parameter values as detailed in the text.

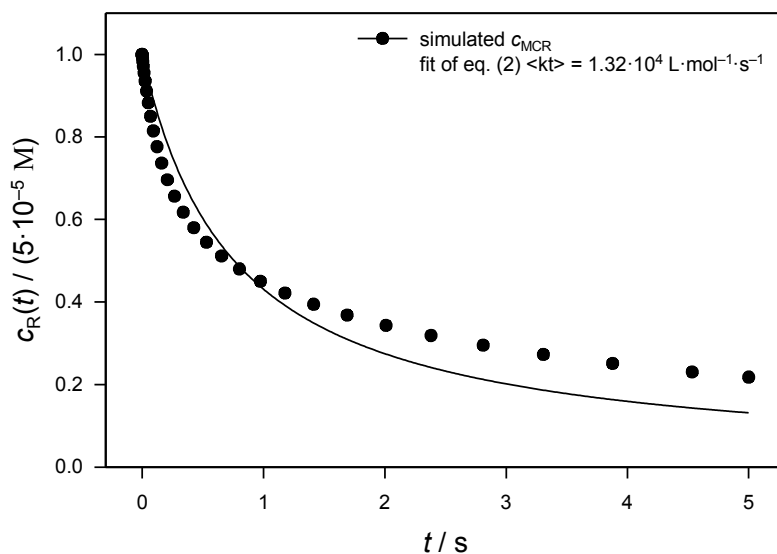


Figure 7. Points: values of MCR concentration, c_R , as a function of time, t , from an SP-PLP simulation with $k_t(\text{A,A}) = 1 \times 10^5 \text{ L mol}^{-1} \text{ s}^{-1}$, $k_t(\text{A,B}) = 1 \times 10^4 \text{ L mol}^{-1} \text{ s}^{-1}$ and $k_t(\text{B,B}) = 5 \times 10^3 \text{ L mol}^{-1} \text{ s}^{-1}$ in a two-state model (see text) with $c_R(0) = 5 \times 10^{-5} \text{ mol L}^{-1}$. Curve: best fit of Equation (2) to the simulation results, yielding k_t of intermediate value, as indicated.

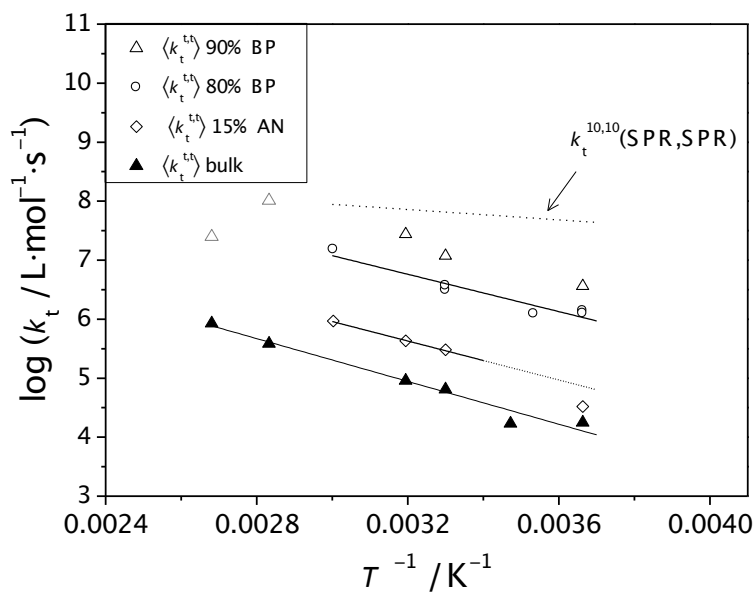


Figure 8. Arrhenius plot of all $k_t(\text{MCR}, \text{MCR})$ values from fitting of Equation (2) to SP-PLP-EPR experiments of this work, where T is absolute temperature. Points: values for (bottom to top) BA macromonomer in bulk (filled triangles), in 15 wt.% acetonitrile (AN) (open diamonds), 80 wt.% butyl propionate (BP) (open circles) and 90 wt.% BP (open triangles). Lines: Arrhenius fits to the data sets (with the exception of the data for 10 wt.% MM; see Table 1 for resulting parameter values), as well as (top line) low-conversion BA values of $k_t^{10,10}(\text{SPR}, \text{SPR})$ (i.e., homo-termination of SPR 10-mers), as obtained in previous SP-PLP-EPR studies.^{10,20}

References

- 1 Junkers, T.; Barner-Kowollik, C. J. Polym. Sci., Polym. Chem. Ed. 2008, 46, 7585-7605.
- 2 Ahmad, N. M.; Heatley, F.; Lovell, P. A. Macromolecules 1998, 31, 2822-2827.
- 3 Chiefari, J.; Jeffery, J.; Mayadunne, R. T. A.; Moad, G.; Rizzardo, E.; Thang, S. H. Macromolecules 1999, 32, 7700-7702.
- 4 Nikitin, A. N.; Hutchinson, R. A. Macromolecules 2005, 38, 1581-1590.
- 5 Nikitin, A. N.; Castignolles, P.; Charleux, B.; Vairon, J. P. Macromol. Rapid Commun. 2003, 24, 778-782.
- 6 Barth, J.; Buback, M. Macromol. React. Eng. 2010, 4, 288-301.
- 7 Buback, M.; Egorov, M.; Junkers, T.; Panchenko, E. Macromol. Rapid Commun. 2004, 25, 1004-1009.
- 8 Barner-Kowollik, C.; Buback, M.; Egorov, M.; Fukuda, T.; Goto, A.; Olaj, O. F.; Russell, G. T.; Vana, P.; Yamada, B.; Zetterlund, P. B. Prog. Polym. Sci. 2005, 30, 605-643.
- 9 Barth, J.; Buback, M.; Hesse, P.; Sergeeva, T. Macromol. Rapid Commun. 2009, 30, 1969-1974.
- 10 Barth, J.; Buback, M.; Hesse, P.; Sergeeva, T. Macromolecules 2010, 43, 4023-4031.
- 11 Zorn, A.-M.; Junkers, T.; Barner-Kowollik, C. Macromolecules 2011, 44, 6691-6700.
- 12 Junkers, T., unpublished results.
- 13 Tanaka, K.; Yamada, B.; Fellows, C. M.; Gilbert, R. G.; Davis, T. P.; Yee, L. H.; Smith, G. B.; Rees, M. T. L.; Russell, G. T. J. Polym. Sci., Polym. Chem. Ed. 2001, 39, 3902-3915.
- 14 Buback, M.; Junkers, T.; Müller, M. Polymer 2009, 50, 3111-3118.
- 15 Junkers, T.; Bennet, F.; Koo, S. P. S.; Barner-Kowollik, C. J. Polym. Sci., Polym. Chem. Ed. 2008, 46, 3433-3437.
- 16 Koo, S. P. S.; Junkers, T.; Barner-Kowollik, C. Macromolecules 2009, 42, 62-69.
- 17 Zorn, A. M.; Junkers, T.; Barner-Kowollik, C. Macromol. Rapid Commun. 2009, 30, 2028-2035.
- 18 Barth, J.; Buback, M.; Hesse, P.; Sergeeva, T. Macromolecules 2009, 42, 481-488.
- 19 Buback, M.; Hippler, H.; Schweer, J.; Vogele, H. P. Makromol. Chem., Rapid Commun. 1986, 7, 261-265.
- 20 Barth, J.; Buback, M.; Russell, G. T.; Smolne, S. Macromol. Chem. Phys. 2011, 212, 1366-1378.
- 21 Barth, J.; Siegmann, R.; Beuermann, S.; Russell, G. T.; Buback, M. Macromol. Chem. Phys. 2012, 213, 19-28.
- 22 Barner-Kowollik, C.; Russell, G. T. Prog. Polym. Sci. 2009, 34, 1211-1259.
- 23 Junkers, T.; Barner-Kowollik, C. Macromol. Theory Simul. 2010, 18, 421-433.
- 24 Smith, G. B.; Russell, G. T. Z. Phys. Chem. (Munich) 2005, 219, 295-323.
- 25 Wulkow, M. Macromol. Theory Simul. 1996, 5, 393-416.
- 26 Smith, G. B.; Russell, G. T.; Heuts, J. P. A. Macromol. Theory Simul. 2003, 12, 299-314.
- 27 Fröhlich, M. G.; Vana, P.; Zifferer, G. J. Chem. Phys. 2007, 127, -.
- 28 Buback, M.; Egorov, M.; Junkers, T.; Panchenko, E. Macromol. Chem. Phys. 2005, 206, 333-341.
- 29 Vana, P.; Yee, L. H.; Barner-Kowollik, C.; Heuts, J. P. A.; Davis, T. P. Macromolecules 2002, 35, 1651-1657.
- 30 Nikitin, A. N.; Hutchinson, R. A. Macromol. Theory Simul. 2006, 15, 128-136.
- 31 Nikitin, A. N.; Hutchinson, R. A. Macromol. Rapid Commun. 2009, 30, 1981-1988.
- 32 Nikitin, A. N.; Hutchinson, R. A.; Wang, W.; Kalfas, G. A.; Richards, J. R.; Bruni, C. Macromol. React. Eng. 2010, 4, 691-706.